0273-2289/90/2425—0103$02.20

Effect of Transient Acid Diffusion on Pretreatment/Hydrolysis of Hardwood Hemicellulose

L. M. TILLMAN,[1] Y. Y. LEE,*[,1] AND R. TORGET[2]

[1]Department of Chemical Engineering, Auburn University, Auburn, AL 36849; and [2]Solar Energy Research Institute, Golden, CO 80401

ABSTRACT

Diffusivities of sulfuric acid in Aspen wood were experimentally determined at various diffusional temperatures and fitted to Arrhenius equations. These equations were subsequently incorporated into a theoretical model to establish the effect of transient acid concentration gradients within a solid substrate during acid-catalyzed hydrolysis of hemicellulose. Total xylose yield was found to decrease for increasing chip size, and this effect was intensified by increasing reaction temperature. Quantitative criteria were established for assessment of transient acid concentration effects upon xylose yield and reaction time at various reaction conditions.

Index Entries: Acid diffusivity; hemicellulose hydrolysis; acid catalyzed; nonuniform acid concentration; biomass size.

INTRODUCTION

Hardwood is one of the least utilized forest resources, and for this reason, it has long been considered a primary feed material for biomass conversion processes. In converting this substrate to the desired final product of ethanol, a number of sequential unit processes are required. The initial stage of such a conversion scheme involves size reduction, acid impregnation, and selective hydrolysis of the hemicellulose fraction at elevated temperatures.

*Author to whom all correspondence and reprint requests should be addressed.

Acid impregnation represents the rate-limiting step of the prehydrolysis stage and, as such, demands an understanding of the transport mechanism involved. At a high moisture content, diffusion, as opposed to migration, of the acid catalyst is the dominant mode of transport. Fukuyama et al. (*1–3*) investigated the diffusion of nonelectrolytes through water-saturated Sitka spruce. These studies emphasized the variation of the diffusion coefficient associated with wood structure. The three diffusional directions identified for wood structures are the longitudinal, tangential, and radial directions. Generally, the longitudinal diffusivity is the dominant factor, and this anisotropic effect has been verified for a variety of wood species by numerous investigators (*4–6*).

In addition to directional dependence, diffusivity through wood is a strong function of temperature. The temperature effect on the diffusion rates of bivalent electrolytes between 20 and 50°C was quantified and fitted to an Arrhenius-type equation in a study by Fukuyama et al. (*7*). A similar approach was utilized by Kumar and Jain (*6*) for the diffusion of boric acid into mango wood. In both the above studies, activation energies of diffusion were calculated and equations presented for the determination of diffusivities at other temperature values. Practical diffusion determinations have been determined for various wood pulping chemicals for both the Kraft (*8*) and sulfite (*9*) processes.

This study was undertaken with the objective of verifying the effect of transient acid diffusion during the prehydrolysis stage of biomass treatment. To this end, the initial phase of this study was focused on determination of the acid diffusivities for fully hydrated Aspen wood at various temperatures. The temperature dependence and the directional difference (anisotropy) of diffusivity, as dictated by wood fiber orientation, were considered. The diffusivity data were further incorporated into a complete hemicellulose hydrolysis reaction model to ascertain the impact of biomass size upon xylose yields and reaction times for specified reaction conditions and what role, if any, nonuniform acid concentration profiles play in the prehydrolysis of Aspen hemicellulose.

EXPERIMENTAL METHODS

Determination of Acid Diffusivity

The experimental set-up for diffusivity determination is presented in Fig. 1. To conduct a diffusivity measurement, a wood slice of known dimensions and grain orientation was fitted with a Viton O-ring and secured between the flanged cell chambers. The platinum-tipped conductivity probe (custom fabricated) was inserted into chamber 1 (distilled/deionized water chamber) and locked into place by a compression fitting. Tubing was attached to allow flow from the acid and water reservoirs (both of which were temperature controlled) into their respective cham-

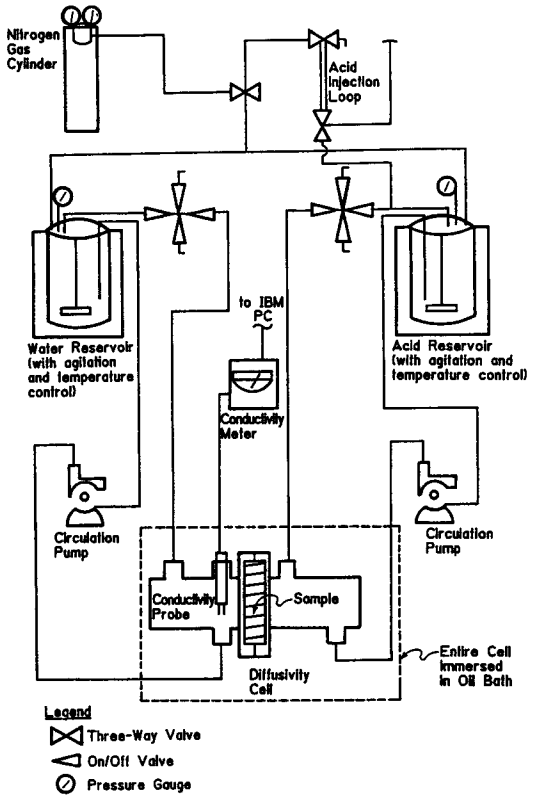

Fig. 1. System schematic for acid diffusivity determination.

bers of the diffusivity cell. The cell chambers are flushed with distilled/deionized water and the sample hydrated for at least 24 h to eliminate any migration effect. Both chambers were emptied, and the two reservoirs were filled with 400 mL distilled/deionized water. The system was put under nitrogen pressure of 20 psig to prevent water vaporization. The diffusivity cell was immersed in a Haake FS-2 oil bath for close temperature control. The oil bath, as well as both reservoir heating mantles, were set at the desired temperature. After thermal equilibration, a known amount of concentrated sulfuric acid was injected into the acid circulation loop to provide a bulk acid concentration of approximately .001*N*. Injection was accomplished via a sample loop applying nitrogen pressure. The analog voltage output from the conductivity meter (Amber Science, model 1051) was amplified and transferred to an IBM Data Acquisition and Control Adapter for input to a BASIC data acquisition program in resident memory of an IBM PC/XT. At the time of injection, the BASIC data acquisi-

tion program was engaged to monitor the change in conductivity in the water circulation loop. The conductivity data were converted to concentrations via a calibration equation. From the slope of concentration vs time, the acid diffusivity was determined by equating the mass transfer through the sample slice to the mass accumulation in chamber 1

$$Q_1 = \text{mass accumulation in chamber 1} = V_1 * (dC_1/dt) \quad (1)$$

$$Q_2 = \text{mass transfer through wood slice} = A * D * (-dC_2/dx) \quad (2)$$

$$Q_1 = Q_2 \quad (3)$$

$$V_1 * (dC_1/dt) = A * D * (-dC_2/dx) \quad (4)$$

where: V_1 = volume of distilled/deionized water (mL); C_1 = concentration of acid in chamber 1 (N); t = time (min); A = surface of wood sample (cm^2); D = acid diffusivity (cm^2/min); C_2 = concentration of acid in wood slice (N); and x = distance across wood sample (cm). The experimentally-determined slope of concentration vs time gave the value of dC_i/dt, found in Eq. (4). For the concentration gradient established across the thickness of the wood slice:

$$-(dC_2/dx) = -(\text{del } C_2/\text{del } x) \quad (5)$$

where: *del* C_2 = (initial C_1 value − bulk concentration); and *del* x = thickness of the wood sample.

Substituting Eq. (5) into Eq. (4)

$$V_1 * (dC_1/dt) = A * D * (-\text{ del } C_2/\text{del } x) \quad (6)$$

Final rearrangement yields

$$D = [(V_1/A) * (\text{exptl. slope}) * (\text{thickness/bulk conc.})] \quad (7)$$

The diffusivity values were calculated from Eq. (7) by linear regression. The diffusivity of Aspen wood varies with temperature, and this variation was modeled by an Arrhenius-type equation such that

$$D = D_o * \exp(-E/RT) \quad (8)$$

MODEL DEVELOPMENT

Kinetic Model

The hydrolysis reaction was modeled as two parallel first order reactions:

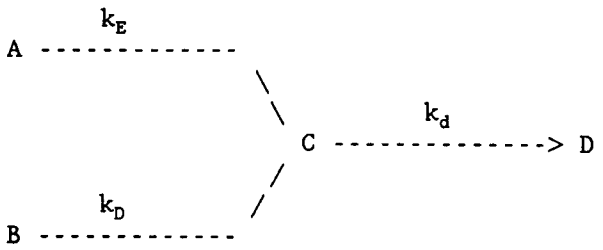

Table 1
Kinetic Parameters Utilized in the Nonuniform Acid Concentration Simulation of Aspen Hemicellulose Hydrolysis

Temp, °C	Fraction "easy" hemicellulose, % of total[a]	Frequency Factors[b]		
		k_{EO}, 1/min	k_{DO}, l/min	k_{dO}, l/min
95	80	1.09×10^{14}	4.52×10^{17}	2.33×10^{12}
120	71	2.37×10^{14}	1.38×10^{18}	2.33×10^{12}
140	77	1.77×10^{14}	4.80×10^{17}	2.33×10^{12}
160	80	1.56×10^{14}	2.03×10^{17}	2.33×10^{12}

[a]Activation Energy (kcal/mol): "easy" reaction = 28; "difficult" reaction = 37; and decomposition reaction = 27.
[b]Acid Exponents: "easy" reaction = 1.54; "difficult" reaction = 1.19; and decomposition reaction = 0.69.

where: A = hemicellulose fraction "easy" to hydrolyze; B = hemicellulose fraction "difficult" to hydrolyze; C = xylose; and D = decomposition products.

Kinetic constants were represented as

$$k_i = k_{io}\, H^{ni}\, \exp(E_i/RT) \tag{9}$$

where: k_i = kinetic constant (1/min); k_{io} = frequency factor (1/min); H = acid concentration (wt. %); n_i = acid concentration exponent; E_i = activation energy (cal/mol); T = temperature (K); and R = gas constant (cal/mol).

A summary of the kinetic parameters utilized in this study are presented in Table 1. These parameters represent a combination of the work of Grohmann et al. for hydrolysis parameters (*10*), Brennan et al. for decomposition parameters (*11*), and Kim et al. for acid concentration exponents for hydrolysis (*12*). The kinetic constants employed at a reaction temperature of 160°C were estimated from the rate constants of Grohmann et al. (*10*). The bulk acid concentration was taken to be .83 wt.% in all cases, a prevalent condition employed for biomass pretreatment studies at SERI.

Transient Acid Diffusion

The acid mass balance within a differential segment of the chip results in the unsteady state diffusion equation

$$\frac{\partial C_s}{\partial t} = D \frac{\partial^2 C_s}{\partial x^2} \tag{10}$$

with boundary and initial conditions of

$$x = 0, \quad \frac{\partial C_s}{\partial x} = 0 \tag{11}$$

$$x = L, \quad -\rho D \frac{\partial C_s}{\partial x} = k (C_s - C_s^B) \tag{12}$$

$$t = 0, \quad C_s = C_s^\circ \tag{13}$$

where: C_s = local acid concentration within biomass chip; C_s^B = bulk acid concentration; C_s^o = initial acid concentration; D = diffusivity; x = position in chip measured from center; L = half thickness of chip; ρ = density; and k = mass transfer coefficient. The analytical solution to Eqs. (10–13) in dimensionless form is as follows

$$\Phi = \sum_{n=0}^{\infty} \frac{2Nu(Nu^2+\lambda_n^2)^{\frac{1}{2}}}{\lambda_n(Nu^2+\lambda_n^2+Nu)} \exp(-\lambda_n^2 t) \cos(\lambda_n z) \tag{14}$$

where: $\Phi = (C_s - C_s^B)/(C_s^o - C_s^B)$ = dimensionless concentration; $\tau = Dt/L^2$ = dimensionless time; $z = x/L$ = dimensionless position; and $Nu = kL/\rho D$ = Nusselt no. for mass transfer (Sherwood no.).

$$\lambda_n \tan(\lambda_n) = Nu \qquad \lambda_n > 0 \tag{15}$$

λ_n = Eigen value. In the computation process, it became evident that Nu values (Nusselt number for mass transfer or Sherwood number) were large enough to render the solution essentially the same as for a boundary condition of $T = C_s^B$ at $x = L$.

Reaction Progression with Transient Acid Diffusion

For the reaction scheme developed, rate constants are a function of acid concentration and reaction temperature. Since the acid concentration is a function of time and the position within the biomass (Eq. (14)), rate constants can be evaluated as a function of time and position such that

$$k_E = k_E(T, C_s) = k_E(t, x)$$
$$k_D = k_D(T, C_s) = k_D(t, x)$$
$$k_d = k_d(T, C_s) = k_d(t, x)$$

The reaction progress in the wood chip is described by

$$-dC_A / dt = k_E C_A \tag{16}$$

$$-dC_B / dt = k_D C_B \tag{17}$$

Table 2
Summary of Acid Diffusivity Values for the Reaction Temperatures of Interest

	Acid Diffusivity (cm^2/s)		
Temp., °C	Radial/Tangential	Longitudinal	Average
95	1.09×10^{-4}	3.35×10^{-4}	2.22×10^{-4}
120	2.21×10^{-4}	5.53×10^{-4}	3.87×10^{-4}
140	3.64×10^{-4}	7.91×10^{-4}	5.78×10^{-4}
160	5.75×10^{-4}	8.33×10^{-4}	7.04×10^{-4}

$$dC_c / dt = k_E C_A + k_D C_B) - k_d C_c \quad (18)$$

with initial conditions of

$$C_A = C_{AO} \quad C_B = C_{BO} \quad C_c = C_{co} \quad \text{at } t = 0 \quad (19)$$

The above equations were put into dimensionless forms and entered into the overall model development. The computer simulation was designed to first determine the acid concentration for values of τ and z. The rate constants were then evaluated at that particular acid level and a given temperature. Finally, with known rate constants, a Runge-Kutta fourth order method was employed to solve the initial value problems of Eqs. (16–19). Simpson's rule was then applied to determine total xylose concentration at any time by integrating over the length of the chip. In essence, the computer simulation provided local xylose and local hemicellulose (easy and difficult) concentration profiles, in addition to the total xylose production for a nonuniform acid concentration distribution, and compared these values to their uniform acid concentration counterparts.

RESULTS AND DISCUSSION

Experimental Acid Diffusivities

The acid diffusivities of fully hydrated Aspen wood were determined via a dynamic method described in the experimental section. With this method, both the longitudinal and radial/tangential diffusivities were determined at temperatures of 25, 50, 70, and 100°C. Arrhenius-type plots were made from the data for each diffusional direction to obtain the following diffusivity-temperature correlation.

$$D_L = .8922 \exp(-5768/RT) \quad (20)$$

$$D_{RT} = 7.018 \exp(-8096/RT) \quad (21)$$

where: D_L = longitudinal diffusivity (cm^2/s); and D_{RT} = radial/tangential diffusivity (cm^2/s). Table 2 presents the diffusivity data for various reaction temperatures. The data confirmed the anisotropy of diffusion, with

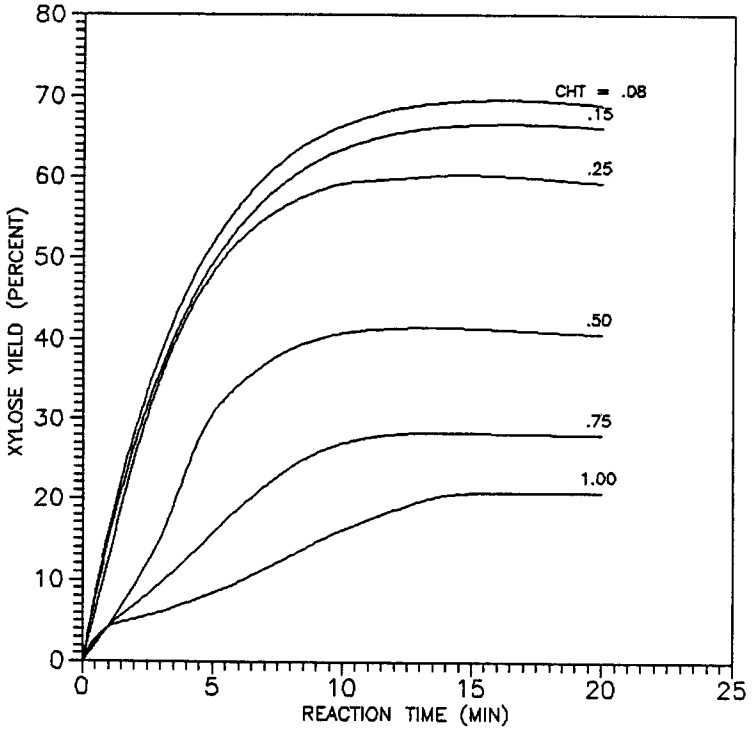

Fig. 2. Xylose yield as a function of reaction time for various chip sizes (hemicellulose hydrolysis at 140°C).

regard to the grain orientation, in that the longitudinal diffusivity is substantially higher than the R/T diffusivity. However, this anisotropic effect, was lessened at high temperatures owing to the more sensitive nature of the R/T diffusivity, with respect to temperature, conforming to the fact that the activation energy for R/T direction is higher than for longitudinal direction, as shown in Eqs. (20) and (21).

The Arrhenius equations, developed for both the longitudinal and R/T diffusivities, yielded activation energies that are comparable to those reported by Kumar and Jain (*6*). In addition, absolute diffusivity values agreed closely with published values using similar substrates (*5–7*). Equations (20) and (21) allowed interpolation or extrapolation to other temperatures of interest and were incorporated into the overall simulation model. Simulation was conducted with an arithmetic average of the two diffusivity values (chipping process is irregular in direction, thereby producing random grain orientations).

Simulation Results

Representative simulation results are presented in Figs. 2 and 3. Figure 2 presents total xylose yield as a function of reaction time for 140°C. It is evident that as chip size is increased, xylose yield drops dramatically,

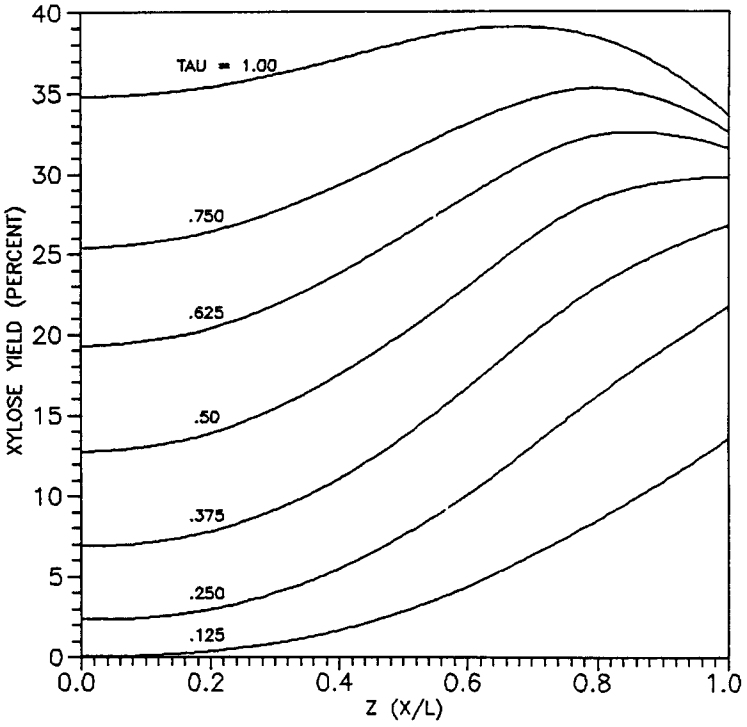

Fig. 3. Local xylose concentration as a function of position for various tau values (hemicellulose hydrolysis at 140°C with CHT = .50 cm).

and this decrease in yield was intensified as the temperature was increased. Figure 3 typifies the results of local xylose yield as a function of position for various τ values. It is to be noted that, for uniform acid concentration, the xylose concentration for each τ should exhibit a flat profile. Figure 3 shows that at early reaction times, the hydrolysis is surface oriented at higher z values. The reaction zone then progressively moves toward the center region as acid catalyst penetrates into it. This surface intensive reaction zone increases its dominance as temperature and chip size increases. Figure 3 also illustrates how decomposition occurs at surface regions (high z values) in direct competition with xylose production at the interior positions. This transient effect tends to drive down the yield from predicted uniform acid concentrations. In all the simulation results, a lag in xylose yield at low z values was exhibited until transient acid concentration effects diminished and uniform acid concentration conditions were established.

Table 3 summarizes the simulation results, including those presented in Figs. 2 and 3. Shown in the table are the ratios of the maximum xylose yield and the reaction time at which maximum xylose yield occurs for uniform vs nonuniform acid concentration conditions. A numerical value of one in the table indicates that, for the stated conditions, acid diffusion is not an influencing factor in overall reaction progression; consequently,

Table 3
Comparison of Maximum Yield and Reaction Time at Maximum Yield for Aspen Hemicellulose Hydrolysis Utilizing an Average Acid Diffusivity

	95°C		120°C		140° C		160°C	
CHT, cm	a	b	a	b	a	b	a	b
0.02	1.00	1.00	1.00	1.00	1.00	1.00	1.00	1.00
0.05	1.00	1.00	1.00	1.00	1.00	1.00	0.98	1.00
0.08	1.00	1.00	1.00	1.00	1.00	1.00	0.96	1.00
0.10	1.00	1.00	0.99	1.02	0.99	1.06	0.93	1.00
0.15	1.00	1.00	0.98	1.05	0.95	1.12	0.85	1.09
0.25	1.00	1.00	0.95	1.08	0.86	1.23	0.67	1.36
0.50	0.99	1.02	0.81	1.18	0.59	1.36	0.36	1.20
0.75	0.97	1.02	0.65	1.29	0.41	1.30	0.26	0.83
1.00	0.94	1.05	0.52	0.83	0.30	1.06	0.19	0.68

a = $(\text{maximum yield})_{\text{nonuniform}}/(\text{maximum yield})_{\text{uniform}}$.
b = $(\text{time@maximum yield})_{\text{uniform}}/(\text{time@maximum yield})_{\text{nonuniform}}$

an assumption of uniform acid concentration is valid. As temperature increased, deviations from a uniform acid concentration assumption appeared at increasingly smaller chip sizes. These initial deviations appeared at chip thicknesses of 1.0, .20, .20, and .10 cm for temperatures of 95, 120, 140, and 160°C, respectively. One may term these values as the critical chip sizes for the respective reaction temperatures, below which the transient acid diffusion effect becomes negligible. We have previously reported on the effect of thermal diffusion upon hemicellulose hydrolysis (*13*). In the study, we have conducted a reaction simulation considering transient thermal diffusion and found the critical chip sizes to be 1.5, .50, and .30 cm for temperatures of 95, 120, and 140°C, respectively. By direct comparison, it is evident that acid diffusion plays a more dominant role during hemicellulose hydrolysis than thermal diffusion for the conditions investigated. Utilizing the criteria set forth in Table 3, as well as the information presented in the complimentary study of thermal diffusion (*13*), the impact of both transport processes may be discerned and utilized as a guide for feed preparation, reactor design, and optimal operation strategy.

CONCLUSIONS

1. The acid diffusivity of Aspen wood was measured by dynamic method for both the longitudinal and radial directions and Arrhenius equations established for temperature dependence.
2. Anisotrophy owing to grain orientation of wood was confirmed

in diffusivity values, as well as in activation energies.
3. A theoretical model was developed to investigate the effects of nonuniform acid diffusion within Aspen wood chip during hemicellulose hydrolysis.
4. Total xylose yield was found to decrease with increasing chip sizes, and this decrease was intensified by increasing reaction temperature.
5. A quantitative guideline was presented to assess transient acid diffusion effects for specific reaction conditions.
6. Acid diffusion, as opposed to thermal diffusion, was shown to exact a greater influence upon hemicellulose hydrolysis.

ACKNOWLEDGMENTS

This work was conducted as part of a research contract with the Solar Energy Research Institute (Contract No. SERI-XK-7070314). Supplementary support was provided by the Pulp and Paper Research and Educational Center of Auburn University.

REFERENCES

1. Fukuyama, M. and Urakami, H. (1986), *Mokuzai Gakkaishi* **32,** 147–154.
2. Fukuyama, M. and Urakami, H. (1982), *Mokuzai Gakkaishi* **28,** 17–24.
3. Fukuyama, M. and Urakami, H. (1980), *Mokuzai Gakkaishi* **26,** 587–594.
4. McGregor, R. P., Peemoeller, H., Schneider, M. H., and Scharp, A. R. (1983), *J. Appl. Polym. Sci.* **37,** 901–909.
5. Bains, B. S. and Kumar, S. (1978), *J. Timber Dev. Assoc. India* **24,** 25–32.
6. Kumar, S. and Jain, V. K. (1973), *Holsforsch. Holzvertwert.* **25,** 21–24.
7. Fukuyama, M., Urakami, H., and Ikuho, I. (1980), *Kyoto-furitsu Daigaku Gakututsu Hokoku. Nogaku* **32,** 101–109.
8. Akhtaruzzaman, A. F. M. and Virkola, N. E. (1979), *Pap. Puu* **61,** 578–580.
9. Surma-Slusarska, B., Rutkowski, J., and Reimschussel, W. (1978), *Pregl. Papier* **32,** 118–125.
10. Grohmann K., Torget, R., and Himmel, M. (1985), *Biotechnol. Bioeng. Symp.* **15,** 59–80.
11. Brennan, A. H., Schell, D. J., Hoagland, W., and Werdene, P. G. (1987), *Ninth Symp. Biotechnol. Bioeng.*, Boulder, CO.
12. Kim, S. B. and Lee, Y. Y. (1986), *Biotechnol. Bioeng. Symp.* **17,** 71–84.
13. Tillman, L. M., Abaseed, A. E., Lee, Y. Y., and Torget, R. (1989), *Biotechnol. Bioeng. Symp.* **20/21,** 107–117.